Available online at www.sciencedirect.com
SCIENCE DIRECT®
Journal of Power Sources 119–121 (2003) 388–392
JOURNAL OF POWER SOURCES
www.elsevier.com/locate/jpowsour

No-flash-point electrolytes applied to amorphous carbon/$Li_{1+x}Mn_2O_4$ cells for EV use

Juichi Arai*

Hitachi Research Laboratory, Department of Battery System Research, MD#260, 1-Material Department, 1-1 Omika-cho 7-chome, Hitachi Ltd., Ibaraki-ken 319-1292, Japan

Abstract

Use of no-flash-point electrolytes (NFEs) containing non-flammable solvent for an amorphous carbon/$Li_{1+x}Mn_2O_4$ cell has been studied. We prepared three NFEs: NFE1 was composed of 1 M (mol dm^{-3}) of $LiN[SO_2C_2F_5]_2$ as supporting electrolyte, and 80 vol.% of methyl nonafluorobutyl ether (MFE) and 20 vol.% of ethyl methyl carbonate (EMC) as solvents; NFE2 was prepared by adding 0.5 M of EC (ethylene carbonate) to NFE1; and NFE3 was prepared by adding 0.1 M of $LiPF_6$ to NFE2. Charge–discharge performance of $Li_{1+x}Mn_2O_4$/Li cells and amorphous carbon/Li cells with NFEs were investigated. The amorphous carbon/$Li_{1+x}Mn_2O_4$ 18650 cells were fabricated and investigated in terms of rate capability and cycle life. NFE2 showed good rate performance. NFE3 showed the best cycle life among the NFE electrolyte cells, though it had only fair rate performance. Electrochemical impedance spectroscopy (EIS), attenuated total reflection infrared (ATR-IR) spectroscopy and X-ray photoelectron spectroscopy (XPS) were measured to study the effect of EC and $LiPF_6$.

Keywords: Electrolyte; No-flash-point; Fluorinated ether; Amorphous carbon anode; $Li_{1+x}Mn_2O_4$ cathode; $LiN[SO_2C_2F_5]_2$

1. Introduction

The combination of an amorphous carbon anode and a $Li_{1+x}Mn_2O_4$ cathode offers higher power and safety than other anode/cathode systems [1]. This cell system provides good safety for the large-size batteries used for EV (electric vehicle) applications. Using a non-flammable electrolyte with the amorphous carbon/$Li_{1+x}Mn_2O_4$ system may realize even greater safety for these large size batteries. We have investigated no-flash-point electrolytes (NFEs) using a non-flammable fluorinated ether (methyl nonafluorobutyl ether (MFE)) in a garaphite/$LiCoO_2$ cell and demonstrated a safety improvement [2]. In the present work, we applied the NFEs to an amorphous carobon/$Li_{1+x}Mn_2O_4$ cell and characterized the cell performance including rate capability and cycle life. The surfaces of the amorphous carbons charged when using NFE electrolytes were analyzed by attenuated total reflection infrared (ATR-IR) spectroscopy and X-ray photoelectron spectroscopy (XPS) to study the effect of electrolyte components on the charge–discharge performance.

2. Experimental

We prepared NFEs by mixing the non-flammable solvent MFE (CH_3–O–C_4F_9, 3 M Company) with ethyl methyl carbonate (EMC, Tomiyama), and dissolving 1 M of LiBETI (lithium bis[pentafluoroethylsulfonyl] imide, $LiN[SO_2C_2F_5]_2$, 3 M Company). The mixing ratio of MFE:EMC was 80:20 vol.% (NFE1). This mixture had no-flash-point according to the JIS 2265-based Cleaveland open cup flash-point test. 0.5 M of ethylene carbonate (EC) were added to NFE1 to obtain NFE2 electrolyte, and 0.1 M of $LiPF_6$ were added to NFE2 to obtain NFE3 electrolyte. 1 M $LiPF_6$-EC/EMC (30:70 vol.%) was used as a reference electrolyte (RE) to evaluate the cell performances.

The anode was made by coating and drying *N*-methyl pyrolidone (NMP) paste containing amorphous carbon (PIC, Kureha) and poly vinylidene fluoride (PVDF) on copper foil. The cathode was prepared in the same way, except the paste contained $Li_{1+x}Mn_2O_4$, PVDF and graphite carbon as electric conducting supporter. PIC/Li and $Li_{1+x}Mn_2O_4$/Li test cells were assembled to investigate charge–discharge capacities and measure electrochemical impedance spectra (EIS). PIC/$Li_{1+x}Mn_2O_4$ 18650 cylindrical cells were also fabricated to examine the rate capability and cycle life.

* Tel.: +81-294-52-7528; fax: +81-294-52-7634.
E-mail address: jarai@hrl.hitachi.co.jp (J. Arai).

0378-7753/03/$ – see front matter © 2003 Elsevier Science B.V. All rights reserved.
doi:10.1016/S0378-7753(03)00258-1

EIS measurements of the test cells were performed using a Solatoron SI1286 potentio-galvanostat and SI1260 impedance/gain-phase analyzer in a frequency range from 1 to 5 mHz. The ATR-IR spectra of amorphous carbon after charge and discharge run were measured by a Bio Rad Digilab FTS-55A using a Ge prism with beam incident angle of 45°, 4 cm^{-1} resolution and 512 scans. X-ray photoelectron spectroscopy (XPS) analysis of the surface of the amorphous carbon electrode was carried out with the VG Scientific ESCALAB 220iXL spectrometer under ultra high vacuum (less than 3×10^{-7} Pa). The surface area measured was 1000 μm ϕ. All samples for ATR-IR and XPS were dried under vacuum at 1×10^{-3} Pa for more than 12 h prior to the measurement to remove residual solvent. An Al Kα X-ray source was used (15 keV, 15 mA). The binding energy of the neutral C 1s peak at 284.6 eV was used as an internal standard to calibrate the binding energy scale.

3. Results and discussion

3.1. PIC/Li and $Li_{1+x}Mn_2O_4$/Li cells

Fig. 1 shows the discharge voltage curves of $Li_{1+x}Mn_2O_4$/Li cells using the NFEs and RE electrolytes. The cells were charged at a constant current ($0.2C = 0.5$ mA) to 4.2 V and discharged to 3 V. The discharge capacity of the cell using NFE1 (MFE/EMC, 84 mAh g^{-1}) was improved by adding EC (NFE2, 97 mAh g^{-1}). NFE2 and NFE3 had sufficient discharge capacities compared to the RE (96.7 mAh g^{-1}) in $Li_{1+x}Mn_2O_4$/Li cell, though NFEs showed a small voltage drop at the beginning of the discharge compared to RE.

Fig. 2 shows the discharge voltage curves of PIC/Li cells using the same electrolytes after being charged with constant current ($0.2C = 1$ mA) and constant voltage of 0 V for 15 h. The cell capacity using NFE1 was 285 mAh g^{-1}. It was 77% of the capacity obtained with RE (370 mAh g^{-1}). Adding EC to NFE1 as NFE2 resulted in a cell capacity of 333 mAh g^{-1}. But, $LiPF_6$ did not improve the capacity; NFE3 discharged only 271 mAh g^{-1} which was even less than that obtained with NFE1. EC reduced the closed circuit voltage (CCV) at the beginning of the discharge leading to a

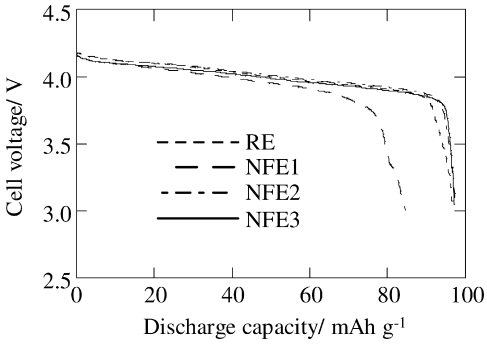

Fig. 1. Discharge voltage curves of $Li_{1+x}Mn_2O_4$/Li cells using the NFEs and RE.

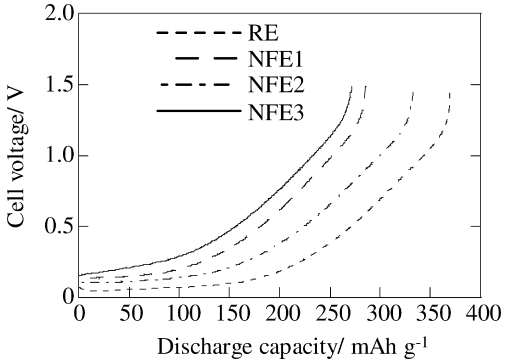

Fig. 2. Discharge voltage curves of PIC/Li cells using the NFEs and RE.

larger capacity than that in the NFE1 cell. However, $LiPF_6$ increased the CCV after charge, indicating that there was an increase of resistance during the charge or the state of the charge did not reach the full capacity of the PIC.

Fig. 3 shows the Cole–Cole plots obtained from the EIS measurements for the PIC/Li cells measured after charge. R_s (resistance corresponding to solution resistance) values in NFE cells were much higher (33, 29, 57 Ωcm^2 for NFE1, NFE2, and NFE3, respectively) than R_s in the RE cell (4 Ωcm^2). This may result in the higher OCV (open circuit voltage) in NFE cells after charge. R_{ct} (charge transfer resistance as diameter of semi-circle) values in NFE cells were also larger (133, 118, 102 Ωcm^2 for NFE1, NFE2, and NFE3, respectively) than R_{ct} in the RE cell (4 Ωcm^2). The order of total resistance ($R_s + R_{ct}$) in these cells agreed well with the order of discharge capacities. EC reduced the cell resistance in NFE cells, but $LiPF_6$ increased it.

3.2. Spectroscopic analysis of amorphous carbon anode

Fig. 4 shows the C 1s XPS spectra for the PIC anode surface after charge in NFE and RE cells. A hydrocarbon

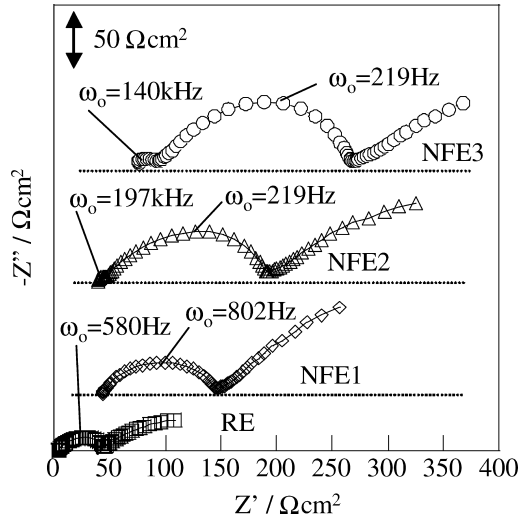

Fig. 3. Cole–Cole plots obtained from EIS measurements for the PIC/Li cells measured after charge.

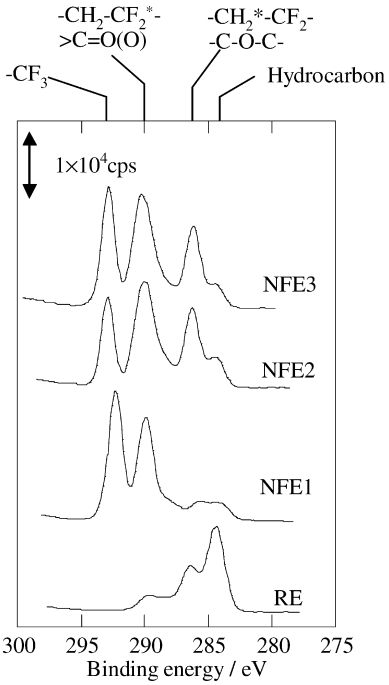

Fig. 4. C 1s XPS spectra for the PIC anode surface after the charge in NFE and RE cells.

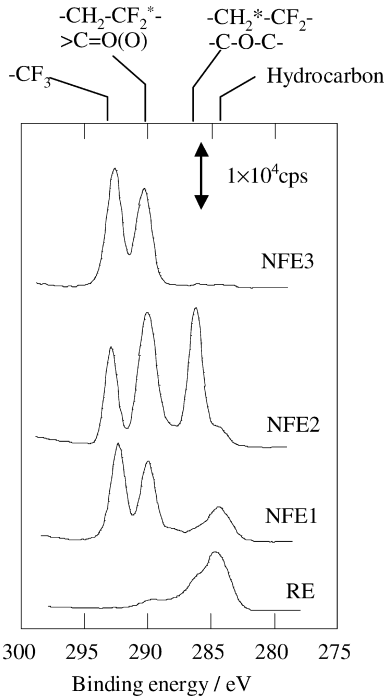

Fig. 5. C 1s XPS spectra for the PIC anode surface after the discharge in NFE and RE cells.

peak (284.5 eV) derived from decomposition of solvents was the dominant peak in the spectrum for the RE cell [3]. The peaks at 290.5 eV (–CF_2) and 293 eV (–CF_3) due to $N[SO_2C_2F_5]_2$ appeared as dominant peaks in the spectrum for the NFE1 cell. Adding EC to NFE1 resulted in the peaks corresponding to solvent decomposition species (hydrocarbon: 284.5 eV, –C–O–C–: 286.5 eV, (O)C=O: 289.5 eV and also >C=O: 287.5 eV) becoming large, while peaks due to $N[SO_2C_2F_5]_2$ decreased in the spectrum for the NFE2 cell. This suggested that EC decomposed faster than EMC and formed solid electrolyte interface (SEI) film on the PIC surface. The SEI film derived from EC resulted in depressing the decomposition or adsorption of $N[SO_2C_2F_5]_2$ and decreasing the cell resistance in the NFE2 cell. The peak intensity ratio (R_I) of the peak at 289.5 to 293 eV in the spectrum for the NFE3 cell decreased somewhat compared to the ratio for NFE2. This suggested that the presence of $LiPF_6$ disturbed the formation of SEI film due to reaction of EC, leading to the larger cell resistance in the NFE3 cell than in the NFE2 cell.

Fig. 5 shows the C 1s XPS spectra for the PIC anode surface after the discharge in NFE and RE cells. The spectrum for the RE cell did not change much, but the peak shape at 284.5 and 286.5 eV became broad. But, the spectra for the NFE cells changed drastically after the discharge. The peaks belonging to $N[SO_2C_2F_5]_2$ decreased and the peak attributed to the hydrocarbon increased in the spectrum for NFE1 cell. This suggested that $N[SO_2C_2F_5]_2$ dissolved into the electrolyte and EMC decomposed to deposit on the anode even during the discharge in the NFE1 cell. The peaks belonging to carbonate species (>C–O and –C–O–C) became large and peaks attributed to $N[SO_2C_2F_5]_2$ (CF_2 and CF_3) decreased. This indicated that EC led to formation of more carbonate species during the discharge and to more formation of the lower resistance SEI film than the other NFEs did. Surprisingly, the peaks due to the carbonate species disappeared and peaks attributed to $N[SO_2C_2F_5]_2$ remained in the spectrum for NFE3. The peak ratio R_I in NFE3 was closed to that in NFE1. This indicated that the peaks at 289.5 to 293 eV were mainly due to the presence of

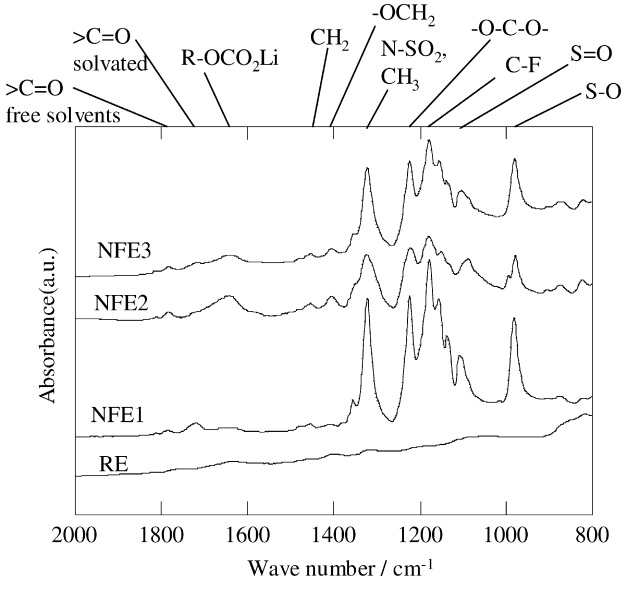

Fig. 6. ATR-IR spectra for the PIC anode after the charge in NFE and RE cells.

$N[SO_2C_2F_5]_2$. The fact suggested that $LiPF_6$ disturbed the stable SEI formation derived from EC.

Fig. 6 shows the ATR-IR spectra for the PIC anode after the charge in NFE and RE cells. Assignments for major peaks are presented in the figure [3,4]. Very small peaks attributed to R–OCO_2Li species (CO_3–Li: 1630, –OCH_2: 1405, and –O–C–O–: 1225 cm^{-1}) were observed in the spectrum for the RE cell. Large peaks belonging to $N[SO_2C_2F_5]_2$ (N–SO_2, S=O, C–F, and S–O) were found in the spectra for NFE cells. There also were a small trace amount of EMC (CH_3: 1320, –CH_2: 1450, >C=O: 1724, and >C=O: 1758 cm^{-1}) and a small amount of R–OCO_2Li species in the spectrum for NFE1. Thus, EMC resulted in some R–OCO_2Li species on the PIC surface, but there was more $N[SO_2C_2F_5]_2$ present. This may limit Li^+ conductivity in the NFE1 cell. The R–OCO_2Li species peaks (especially at 1630 cm^{-1}) increased and $N[SO_2C_2F_5]_2$ peaks decreased in the spectrum for NFE2 cell. EC gave a large amount of R–OCO_2Li, improving the conductivity of NFE2 cell. The spectrum for NFE3 cell did not differ much from that for NFE2 cell, the same tendency as seen in the XPS analysis.

To see the effect of LiPF6, the ratios of P/Li in atomic % (R_{PLi}) were compared by XPS analysis for the surface of anode from the RE cell and NFE3 cells. The R_{PLi} for the RE cell anode was 0.045 (1.8/40.8), while the R_{PLi} for NFE3 cell was 0.03 (0.4/13.2). A larger than expected R_{PLi} was found in the NFE3 specimen, considering the $LiPF_6$ concentration in electrolyte (1 M in RE and 0.1 M in NFE3). This suggested that $LiPF_6$ in the NFE3 (MFE/EMC) had higher reactivity toward the PIC surface than that in the RE (EC/EMC).

3.3. PIC/ $Li_{1+x}Mn_2O_4$ 18650 cell performances

Fig. 7 shows the rate capabilities of PIC/ $Li_{1+x}Mn_2O_4$ 18650 cylindrical cells using NFEs and RE at 20 °C. The cells were charged with constant current (0.2*C*≡160 mA) and constant voltage (4.2 V) to current cut-off limit of 10 mA, and discharged under constant current (0.2*C*) to 2.7 V. The cell discharged 745 mAh at 0.2*C* and 670 mAh at 3*C* (90% of the capacity compared to 0.2*C*) when RE was used. At 0.2*C*, NFEs had sufficient capacities, 753 mAh for NFE1, 754 mAh for NFE2 and 734 mAh for NFE3. Thus, the charge–discharge performance in the anode did not seem to affect the cell capacity in 18650 cells at a low current. At 3*C*, NFE1 discharged 509 mAh, 67% (3*C*/0.2*C*), NFE2 discharged 624 mAh, 82% and NFE3, 575 mAh 78%. EC improved the rate capability of NFE1, but $LiPF_6$ depressed the rate capability as seen in the performances of PIC/Li cells. Thus, the charge–discharge properties in the anode must influence the cell rate capability. The rate capability was in the order RE > NFE2 > NFE3 > NFE1.

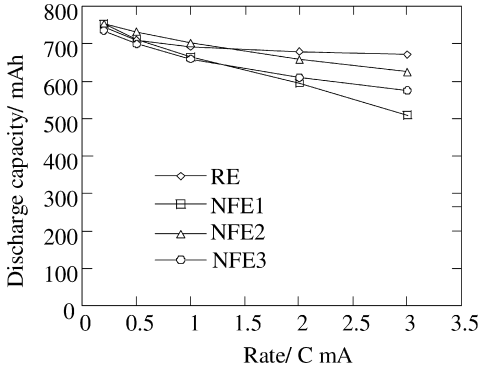

Fig. 7. The rate capabilities of the PIC/ $Li_{1+x}Mn_2O_4$ 18650 cylindrical cells using NFEs and RE at 25 °C.

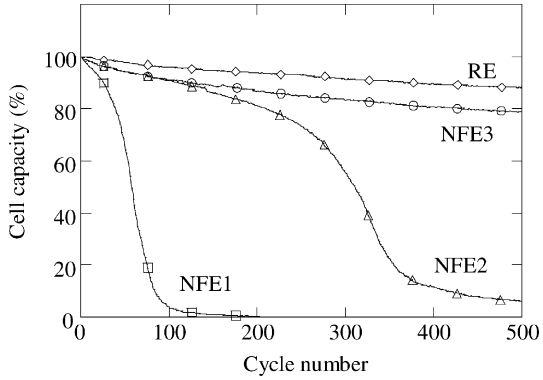

Fig. 8. Cycle life for the PIC/ $Li_{1+x}Mn_2O_4$ 18650 cylindrical cells using NFEs and RE at 25 °C.

Fig. 8 shows the cycle life for the PIC/ $Li_{1+x}Mn_2O_4$ 18650 cylindrical cells using NFEs and RE at 25 °C. The capacity of the NFE1 cell decreased suddenly after around 20 cycles. NFE2 behaved the same as NFE1 did after around 200 cycles. The NFE3 cell kept more than 79% of its initial capacity up to 500 cycles, though this was unsatisfactory when compared to the cycle life of the RE cell. The causes of this improvement given by NFE electrolytes must still be investigated from the view-points of (i) the change of anode resistance due to surface film growth and (ii) the anion ($N[SO_2C_2F_5]_2^-$) reactivity toward Al current collector [3,5,6].

4. Conclusions

The use of NFEs (non-flammable electrolyte) for large size lithium secondary batteries employing an amorphous carbon (PIC)/ $Li_{1+x}Mn_2O_4$ system was investigated. The charge–discharge capacities of both PIC/Li and $Li_{1+x}Mn_2O_4$/Li cells using NFE1 (1 M LiBETI MFE/EMC (80:20 vol.%)) were improved by adding EC (NFE2). The formation of an alkyl carbonate species in solid electrolyte interface film was clearly detected by XPS and ATR-IR analysis for the PIC/Li cell using NFE2. Adding $LiPF_6$ to NFE2 prolonged the cycle life of the PIC/ $Li_{1+x}Mn_2O_4$ cell, but the rate capability was depressed. The amount of $LiPF_6$ should still be optimized in order to achieve good rate capability and cycle life of NFEs for PIC/ $Li_{1+x}Mn_2O_4$ cell.

References

[1] K. Tamura, T. Horiba, T. Iwahori, J. Power Sources 81–82 (1999) 156.
[2] J. Arai, J. Appl. Electrochem. 32 (2002) 1071.
[3] K. Kanamura, T. Umegaki, S. Shiraishi, M. Ohashi, Z. Takehara, J. Electrochem. Soc. 149 (2002) A185.
[4] D. Aurbach, O. Chusid, I. Weissman, P. Dan, Electrochim. Acta 41 (1996) 747.
[5] L. Péter, J. Arai, J. Appl. Electrochem. 29 (1999) 1053.
[6] L. Péter, J. Arai, H. Akahoshi, J. Electroanal. Chem. 482 (2000) 125.